

Submerged Porous Plate Wave Absorber

W.T. PARK*, S.H. LEE* AND S.T. KEE*

*Dept. of Civil Engineering, Seoul National University of Technology, Seoul, Korea

KEY WORDS: Wave Absorber, Wave-Trapping, Horizontal Porous Plate, Standing Wave

ABSTRACT : *In the present paper, the wave absorbing performance of the fully submerged horizontal porous plates has been investigated, numerically and experimentally. The submerged porous system is composed of multi-layered horizontal porous plates that are clamped at the vertical setwall, which are slightly inclined and placed vertically, in parallel, with spacing. The hydrodynamic interaction of incident waves with the rigid porous multi-layered plates was formulated within the context of linear wave-body interaction theory and Darcy's law. In order to validate the effectiveness of the present computing code, the numerical results were compared with the analytical and experimental results. It is found that triple horizontal porous plates with slight inclination, if properly tuned for wave energy dissipation against the standing waves in front of the vertical wall, can have high performances in reducing the reflected wave amplitudes against the incident waves over a wide range of wave frequency.*

1. INTRODUCTION

The wave absorbing breakwater inside the sheltered region is one of the current engineering advancements in port design, designed to provide a further calm basin to insure safer and more efficient port operation, ship berthing, and navigation within inner harbors (Yip and Chwang, 2000). In view of this, many researchers have been particularly interested in the interaction between the water waves and porous structures. Based on linear water wave theory, a series of study can be traced back to the analysis of wave motion over a submerged porous plate by using a boundary element method (Yu and Chwang, 1994). It was found that a plate with proper porosity could significantly suppress the wave reflection. The water wave reflection by a vertical wall with a horizontal submerged porous plate was investigated by Wu et al. (1998), using the eigenfunction expansion method, and found that the larger plate with proper porosity behaves similarly to a wave absorber, which can suppress the wave amplitude on the vertical wall surface and reflected waves. The combination of a perforated wall and a submerged horizontal plate has been investigated by Yip and Chwang (2000), and found that the size of a wave chamber can be reduced by the presence of the internal horizontal plate which generates the shorter wavelength. Cho and Hong (2004) investigated the performance of a wave absorbing system with an inclined porous plate, using a multi-domain boundary element method, and checked its validation through

the comparison with experimental results. It was found that an inclined porous plate produces a higher wave absorbing efficiency, for the inclined angle range between 10° and 20° , compared to a horizontal one.

This series of previous research results motivates us to investigate the phenomenon of the wave energy dissipation over the inclined porous plates in front of the vertical wall, and determine the optimal system that has better performance, especially in the long wave region. Based on the wave motion of local standing wave, one inclined porous plate and two reversely inclined plates have been used for further wave energy dissipation by the trapped waves in front of the vertical wall.

To assess the efficiency of triple horizontal porous plates, a two-dimensional multi-domain formulation was carried out in the context of linear wave body interaction theory and Darcy's law. It is assumed that the ratio of thickness of the plates to the wavelength is small enough to neglect its effects. The hydrodynamic interaction of incident waves with the rigid porous multi-layered bodies was determined by the distribution of the simple sources along the boundaries, which satisfies the Laplace governing equation in each fluid domain. The accuracy and convergence of the developed multi-domain boundary element program were checked based on the energy-conservation formula for a limiting case. The numerical results were further verified through comparison with the experimental result in a two-dimensional wave tank. The numerical predications for the selected optimized model, through a series of parametric study, were generally in good agreement with experimental results.

It is found that triple horizontal porous plates with slight

inclination can, if properly tuned for wave trapping to the coming waves, have high performance in reducing the reflected wave amplitudes against the incident waves, over a wide range of wave frequency. It is also found that the permeability on plates significantly reduce hydrodynamic forces by energy dissipation through fine pores, based on the fluid viscosity, which subsequently further reduces the reflected wave height. Some results are particularly interesting for possible application in a caisson type breakwater design.

2. THEORY AND NUMERICAL METHOD

2.1 Governing Equations

The general features of the proposed system are depicted in Fig. 1. The slightly inclined, horizontal porous plate is fixed into the vertical wall. A Cartesian coordinate system (x, y) is defined, with x measured in the direction of wave propagation from a point at the vertical wall, and y measured upward from the still water level. A monochromatic incident, regular, small amplitude wave train of half height A and angular frequency ω propagates towards the breakwater in water of constant depth h , as shown in fig. 1. If the fluid is assumed to be an ideal fluid, which

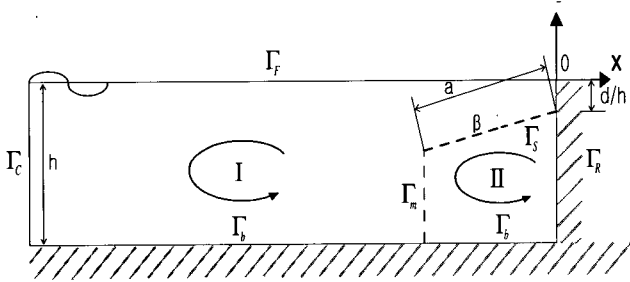


Fig.1 Definition sketch and integration domains for a proposed system.

is incompressible, inviscid, and irrotational, then the fluid motion can be described by velocity potential Φ , which satisfies the Laplace equation $\nabla^2 \phi_l = 0$ within the fluid regions $(\Omega_l, l=1,2)$. In addition, the wave amplitude is assumed sufficiently small enough for linear wave theory to apply. Consequently, Φ is subject to the usual boundary conditions: linearized free surface (Γ_F), rigid structures (Γ_S, Γ_R), bottom (Γ_b), and approximated far field conditions (Γ_C) (see, for example, Sarpkaya and Isaacson, 1981). Thus, ϕ may be expressed in the following form:

$$\Phi(x, y, t) = \text{Re}[\{\phi_o(x, y) + \phi_l(x, y)\}e^{ikx-i\omega t}] \quad (1)$$

where ϕ_o is the well known incident potential, and can be written as:

$$\phi_o = \frac{igA}{\omega} \frac{\cosh k(y+h)}{\cosh kh} e^{ikx} \quad (2)$$

Also, $\text{Re}[\]$ denotes the real part of a complex expression $i = \sqrt{-1}$, t denotes time, and k is the wave number, propagating in the positive x direction, and is the positive real solution of the dispersion equation $\omega^2 = kg \tanh kh$ with g being the gravitational constant. The time independent unknown complex disturbance velocity potentials ϕ_1, ϕ_2 in two fluid domains (see Fig. 1) satisfy the Laplace equation and the following linearized free surface (Γ_F), bottom (Γ_b), structure (Rigid wall) (Γ_R), and radiation (Γ_C) conditions:

$$-\omega^2 \phi_l + g \frac{\partial \phi_l}{\partial y} = 0 \quad (\text{on } \Gamma_F) \quad (3)$$

$$\frac{\partial \phi_l}{\partial n} = 0 \quad (\text{on } \Gamma_b) \quad (4)$$

$$\frac{\partial \phi_o}{\partial n} = -\frac{\partial \phi_s}{\partial n} \quad (\text{on } \Gamma_R) \quad (5)$$

$$\lim_{x \rightarrow -\infty} \left(\frac{\partial \phi}{\partial x} + ik\phi \right) = 0 \quad (\text{on } \Gamma_C) \quad (6)$$

2.2 Porous Plate Boundary Condition

The required linearized kinematic boundary condition on the surface of the porous structure may be developed, based on the formulation of Wang and Ren (1993).

$$\frac{\partial \phi_1}{\partial x} = -\frac{\partial \phi_2}{\partial x} = u(y) \quad \text{on } (\Gamma_S) \quad (7)$$

where $u(y)$ is spatial component of the normal velocity of the fluid flow passing through a thin porous media, which is assumed to obey Darcy's law. The porous flow velocity inside of a plate with fine pores is linearly proportional to the pressure difference between either side of the thin membrane. Therefore, it follows that

$$u(y) = \frac{B}{\mu} \rho i \omega (\phi_1 - \phi_2) \quad (8)$$

where B is the constant, permeability having dimension of a length, μ is the constant coefficient of dynamic viscosity, and ρ is the constant, fluid density. The non dimensional porosity parameter G , commonly called Chwang's parameter (Chwang, 1983), is employed as follows:

$$G = 2\pi\rho\omega B/k\mu \quad (9)$$

This parameter can be regarded as a sort of Reynolds number, representing the effects of both viscosity and porosity, considering the phase velocity of incident wave (ω/k) and a measure of porosity with length dimension (B).

2.3 Matching Boundary Condition

In order to match the two solutions on the fictitious boundary between domain I and II, ϕ_1 and ϕ_2 , the scattered potentials must also satisfy the following linearized boundary conditions, based on the continuity of pressure and normal velocity:

$$\phi_1 = \phi_2, \quad \frac{\partial\phi_1}{\partial n} = -\frac{\partial\phi_2}{\partial n} \quad (\text{on } \Gamma_m) \quad (10)$$

2.4 Boundary Integral Equation

A boundary integral equation method, using simple sources along the entire boundary, is developed to solve the above boundary value problem. Although the use of the free surface Green function is known to be more efficient for the case of a flat bottom, the present method is adopted, since it can be used for arbitrary bottom topography and can easily be extended to the nonlinear time domain problem. One auxiliary vertical boundary (Γ_c) is located sufficiently far from the edge of the horizontal plate that the radiation condition (5) is valid.

In each of the fluid regions, Green's theorem is applied to the unknown complex velocity potentials ϕ_1, ϕ_2 and the Green function of

$$G = \ln\sqrt{(x-x')^2 + (y-y')^2}$$

where (x, y) and (x', y') are the field and source points, respectively, and the boundary conditions (3) (10) are imposed, the integral equations in each fluid domain can be written as:

$$\begin{aligned} & C\phi_1 + \int_{\Gamma_f} \left(\frac{\partial G}{\partial n} - vG\right)\phi_1 d\Gamma + \int_{\Gamma_c} \left(\frac{\partial G}{\partial n} - ikG\right)\phi_1 d\Gamma + \int_{\Gamma_b} \phi_1 \frac{\partial G}{\partial n} d\Gamma \\ & + \int_{\Gamma_m} \left(\phi_1 \frac{\partial G}{\partial n} - G \frac{\partial\phi_1}{\partial n}\right) d\Gamma + \int_{\Gamma_r} \phi_1 \frac{\partial G}{\partial n} d\Gamma + \int_{\Gamma_s} \left(\phi_1 \frac{\partial G}{\partial n} + G(i\rho\omega \frac{b_0}{\mu}(\phi_1 - \phi_2))\right) d\Gamma \\ & = - \int_{\Gamma_r} G \frac{\partial\phi_0}{\partial n} d\Gamma - \int_{\Gamma_s} G \frac{\partial\phi_0}{\partial n} d\Gamma \end{aligned} \quad (12)$$

$$\begin{aligned} & C\phi_2 + \int_{\Gamma_b} \phi_2 \frac{\partial G}{\partial n} d\Gamma + \int_{\Gamma_r} \phi_2 \frac{\partial G}{\partial n} d\Gamma + \int_{\Gamma_s} \left(\phi_2 \frac{\partial G}{\partial n} - G(i\rho\omega \frac{b_0}{\mu}(\phi_2 - \phi_1))\right) d\Gamma \\ & + \int_{\Gamma_m} \left(\phi_2 \frac{\partial G}{\partial n} + G \frac{\partial\phi_2}{\partial n}\right) d\Gamma = - \int_{\Gamma_r} G \frac{\partial\phi_0}{\partial n} d\Gamma - \int_{\Gamma_s} G \frac{\partial\phi_0}{\partial n} d\Gamma \end{aligned} \quad (13)$$

where the infinite depth wavenumber is $v = \omega^2/g$, and C is the solid angle constant.

The above boundary and integral equation can be expanded to 4 fluid domains, which have 3 inclined porous plates fixed into the vertical wall.

3. EXPERIMENTS

In order to validate the theory and numerical procedure developed in the preceding section, we conducted a series of experiments using our two dimensional wave tank, located in the civil engineering laboratory building at Seoul National University of Technology. The glass walled tank is 25 m long, 1 m wide, and 1 m deep, and is equipped with a piston-type wavemaker that is capable of producing regular and irregular waves with periods ranging from 0.25 to 5.6 sec and maximum height of 25 cm.

The wave elevation was measured with a resistance wave gauge, which has an accuracy of ± 0.1 cm. Calibration of wave gauge was completed before and after each set of experiments. A probe measuring incident and reflected wave heights was placed at 11m from the wavemaker, respectively. The wave absorber model was placed at 22m from the wavemaker. Regular waves were generated by a user defined, time voltage input to the wavemaker. The wave period range used in our experiments was from 0.85 to 5. The resonance of the cross wave occurs when $kB = 2n\pi$, where n =integer and B =ank width. The wave periods used in our experiments were greater than this resonant period. The wave heights used in our experiments ranged from 3cm to 6cm. The time series of generated regular waves was sinusoidal, with the beginning and end of the series attenuated in amplitude. All tests were

conducted at the water depth of 0.6m.

The model consisted of a porous plate or multi layered triple porous plates fixed in the vertical wall. The stainless still plates were 0.6m in length and the same porosity $P = 0.0816$ ($G = 3.73$), consisting of many small and regularly punched holes.

The signal of the incident wave train was obtained as it passed the probe toward the membrane breakwater. Then, the reflected wave train was recorded as the reflected waves passed the probe, again, in the opposite direction. After averaging the wave heights for the incident and reflected waves, the reflection coefficient R_f can be calculated from the ratio of the averaged reflected wave height to the averaged incident wave height. For this, we selected only the uniform part of the signal. In some cases, when reflected wave heights are small, they cannot be clearly differentiated from the attenuating incident wave train. Therefore, for each wave period, we calculated the group velocity to estimate the arrival time of the front of the incident and reflected wave trains. Wave generation time was also controlled, based on this group velocity estimation. We also observed that reflected waves were repeatedly reflected from the wavemaker. In order to minimize the effects of multiple reflections, the fixed single probe method was adopted, as opposed to the moving single probe method and three probe method (Isaacson, 1991). Due to the insufficient length of our tank, the present method is not very effective for very long waves. In other words, for longer wave periods, the number of uniform waves dwindles; hence, it is not highly reliable.

4. RESULTS AND COMMENTS

A boundary integral equation method, based on the distribution of simple sources along the entire boundary, is developed for the numerical solution. The two vertical truncation boundaries are located sufficiently far from the side edge of structures, usually 3~4 times of water depth away, such that the far-field boundary condition is valid, i.e. to ensure that the exponentially decaying local standing wave effect is negligible.

The convergence of the numerical results with the increase of the number of segments is shown in Fig. 2, for horizontal porous plate with $G=5$ and submergence depth $d/h=0.1$ at the vertical wall. Fig. 2 demonstrates the variation of the reflection coefficients R_f versus the relative plate length a/λ

for different number of segments, NE1, NE2, along a closed boundary of the fluid domains and an analytic solution. The numerical results uniformly approach towards the analytic solution, as the number of segments is increased. The analytic solution has been developed by Cho and Hong (2004), based on the eigenfunction expansion method.

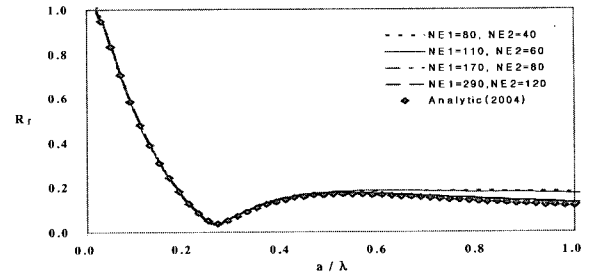


Fig. 2 Convergence checked with number of elements and a comparison of numerical method with analytic solutions for a system with $G=5$, $d/h=0.1$, $a/h=1.0$

Another convergence test, using the numerical results for varying non dimensional porous parameter $G=0 \sim 20$, is shown in Fig. 3. The reflection coefficient is approaching unity for impermeable plate $G=0$ with negligible small differences. The impermeable plate reflects almost all incident waves without energy loss. As the porous coefficients increased, those reflection coefficients are gradually decreased to a certain porosity coefficient $G=5$ for a relatively wide range of a/λ . For a relatively larger porosity, such as $G=10 \sim 20$, the reflected waves gradually increased; thus, an optimal value of G may exist along the relative plate length a/λ . The horizontal plate with smaller porosity absorbs almost completely at the resonance frequency; however, it has generally poor performance for a wide range of relative plate length a/λ . The wave absorber system ($G=5$) shows an outstanding performance, except in the long wave region.

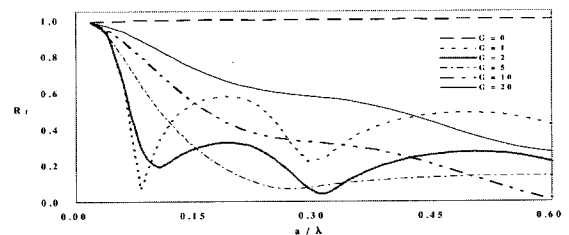


Fig. 3 Variation of reflection coefficients versus a/λ for various value of G for $d/h=0.1$, $a/h=1.0$, $\beta=0^\circ$

The wave energy generally is focused near the free surface; thus, the optimized submergence depth of a horizontal plate may exist, as shown in Fig. 4, based on the wave trapping effects inside of the porous system at the vicinity of the vertical wall.

For the progressive wave energy dissipation through fine pores on the plate, the slightly inclined porous plate might have an advantage, creating a gradually decreased water depth. Therefore, the variation of reflection coefficients has been checked for various angles between the horizontal axis and plate at the vertical wall, as shown in Fig. 5. An optimum angle may exist approximately between $\beta = 7^\circ$ and $\beta = 10^\circ$. For a relatively large angle, the efficiency of wave absorber becomes poor for a wide range of frequency, especially for the relatively long wave regions.

Based on the results of the analysis, as shown in Fig. 3, 4, 5, we can reach a tentative conclusion that a system with proper porosity, submergence depth, and inclined

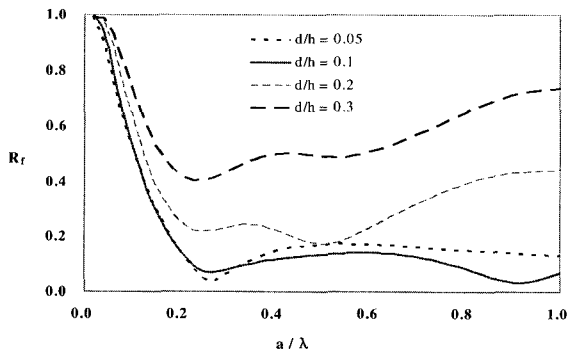


Fig. 4 Variation of reflection coefficients versus a/λ for various value of d/h for $d/h = 1.0$, $\beta = 0^\circ$, $G = 5$

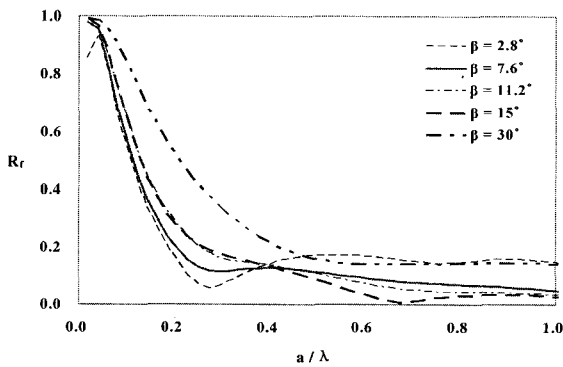


Fig. 5 Variation of reflection coefficients versus a/λ for various value of β for $d/h = 0$, $a/h = 1.0$, $G = 5$

angle significantly influences the performance as a wave absorber. It is interesting to note that the efficiency of the wave energy dissipation, using a horizontal plate with a proper porosity, relatively depends on the water wave velocity and exclusion length of standing waves in front of the wall. Thus, more submerged inclined porous plates need to be added to a single system in order to further dissipate long wave energy.

In order to validate the numerical results and the above discussions, a series of experiments have been conducted in the 2 D wave tanks. The performances of a slightly inclined porous plate and triple multi layered inclined porous plate had been checked with those experimental results, as shown in Fig. 6a and 6b. In Fig 6b, those two reversely inclined porous plates are installed in parallel to improve efficiency of water wave energy dissipation for relatively long waves and to avoid system resonance that aggravates the performance. The reflection coefficients versus the relative plate length a/λ for a single porous plate with $P = 0.0816$ ($G = 3.73$) and $\beta = 7.6^\circ$ are plotted for different wave heights from 1.5cm to 3cm, as shown in Fig 7. As can be seen from this figure, the numerical prediction agrees very well with experimental results, with the exception of the overestimated regions around of $a/\lambda = 0.2$.

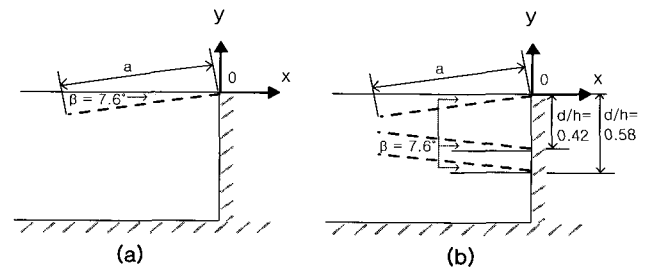


Fig. 6 Definition sketch for two proposed system of experiments

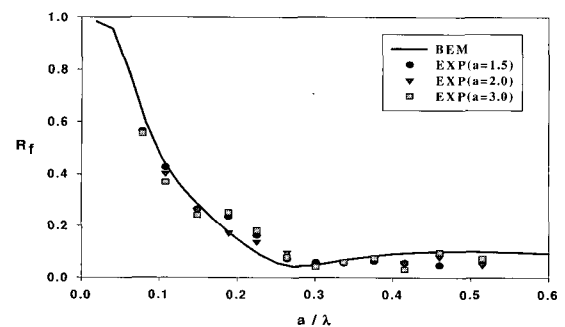


Fig. 7 Comparison of numerical and experimental results for an inclined porous plate for $a/h = 1.0$, $d/h = 0$, $G = 3.73$, $\beta = 7.6^\circ$ for different wave heights

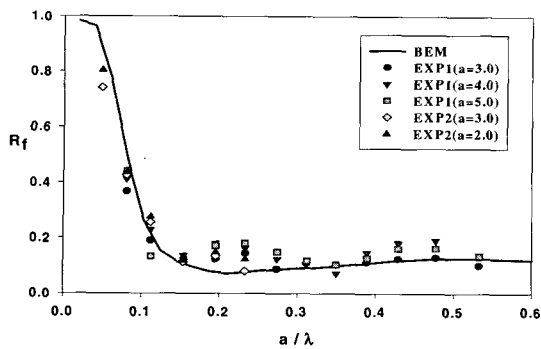


Fig. 8 Comparison of numerical and experimental results for triple multi layered and inversely inclined porous plates for $a/h=1.0$, $G=3.73$, $(d/h)_i = 0., 0.42, 0.58$, $\beta_i=7.6^\circ$, $i=1, 2, 3$

In order to investigate the validation of the proposed model for a wave absorption system with good performance, suppressing significantly the reflected waves, especially in long wave regions, two experiments have been conducted for different wave heights and for large wave periods. Fig. 8 shows the reflection coefficients versus relative plate length a/λ for triple, multi-layered, and inversely-inclined porous plates with $P=0.0816$ ($G=3.73$) and $\beta_i=7.6^\circ$, $i=1,2,3$ for different wave heights from 2cm to 5cm, and up to 5sec wave periods, in 60cm water depth, in order to investigate the validation of the developed theory in long wave regions. Both the numerical and experimental results agree well. Thus, based on the comparison between Fig. 7 (single plate) and Fig. 8 (tuned multi layered plates) in the long wave regions, we can conclude that a well tuned system, using major parameters affecting the performance, can be a very effective wave absorber for the wide range of incident wave frequencies, if the system efficiently utilizes the wave energy dissipation mechanisms of standing waves in front of the vertical wall.

SUMMARY AND CONCLUSIONS

The interaction of monochromatic incident waves with a porous breakwater, containing multi-layered and slightly inclined horizontal porous plates, was investigated in the

context of 2D linear wave theory, based on Darcy's law, due to fluid viscosity through fine pores. A properly adjusted 2 D B.E.M. code has been used to determine the major parameters influencing its performances. The developed program for a porous problem has been checked against the analytic solution for limited cases, and further checked with a series of experimental results, and was found to be in good agreement. It was found that a properly tuned system has an excellent efficiency of wave energy dissipation, in the wide range of wave frequencies, based on the water wave dynamics in front of the vertical wall, since water wave velocity and exclusion length of standing waves significantly interact with horizontal porous plates.

REFERENCES

- Cho, I.H. and Hong, S.W. (2004). "Development of a Wave Absorbing System using an Inclined Punching Plate", J. Ocean Engineering and Technology, Vol 18, No 1, pp 1-6.
- Chwang, A.T. (1983). "A Porous Wavemaker Theory", J. Fluid Mech., Cambridge, U.K., Vol 132, pp 395-406.
- Isaacson, M. (1991). "Measurement of Regular Wave Reflection", J. Waterway, Port, Coastal & Ocean Engineering, ASCE, Vol 117, No 6, pp 553-569.
- Sarpkaya, T. and Isaacson, M. (1981). Mechanics of Wave Forces on Offshore Structures, Van Nostrand Reinhold, New Turk:
- Wang, K.H. and Ren, X. (1993). "An Effective Wave-Trapping System", Ocean Engineering, Vol 21, pp 155-178.
- Wu, J., Wan, Z. and Fang, Y. (1998). "Wave Reflection by a Vertical Wall with a Horizontal Submerged Porous Plate", Ocean Engineering, Vol 25, No 9, pp 767-779.
- Yip, and Chwang, A.T. (2000). "Perforated Wall Breakwater with Internal Horizontal Plate", J. Engrg. Mech., ASCE, Vol 126, No 5, pp 533-538.
- Yu, X. and Chwang, Allen T. (1994). "Water Waves above Submerged Porous Plate", J. Engrg. Mech., ASCE, Vol 120, pp 1270-1281.

2005년 3월 29일 원고 접수

2005년 7월 28일 최종 수정본 채택